

Electrohydrodynamic behaviors of droplet under a uniform direct current electric field*

Zi-Long Deng(邓梓龙)¹, Mei-Mei Sun(孙美美)¹, and Cheng Yu(于程)^{1,2,†}

¹Key Laboratory of Energy Thermal Conversion and Control of Ministry of Education, School of Energy and Environment, Southeast University, Nanjing 210096, China

²Department of Mechanical Engineering, University of Hawaii at Manoa, Honolulu 96822, USA

(Received 1 August 2019; revised manuscript received 22 November 2019; accepted manuscript online 7 January 2020)

The electrohydrodynamic behaviors and evolution processes of silicone oil droplet in castor oil under uniform direct current (DC) electric field are visually observed based on a high-speed microscopic platform. Subsequently, the effects of different working conditions, such as electric field strength, droplet size, *etc.*, on droplet behaviors are roundly discussed. It can be found that there are four droplet behavior modes, including Taylor deformation, typical oblique rotation, periodic oscillation, and fracture, which change with the increase of electric field strength. It is also demonstrated that the degree of flat ellipse deformation gets larger under a stronger electric field. Moreover, both of the stronger electric field and smaller droplet size lead to an increase in the rotation angle of the droplet.

Keywords: DC electric field, droplet, deformation, rotation

PACS: 47.55.D-, 68.05.-n, 47.65.-d

DOI: 10.1088/1674-1056/ab6835

1. Introduction

The electrohydrodynamic behavior of droplets under the electric field plays an important role in a wide range of areas from science to industry, such as electrospray, electrostatic atomization, jet fracture charge, electric defogging, electric demulsification, ink jet printing, electrohydrodynamic air pumps, and beyond.^[1–5] Different droplet behaviors have been found in the presence of external electric field, including directional movement, deformation, rotation, fracture, and polymerization.^[6–10] These complex electrodynamic behaviors attract many researchers' interests.^[11,12] The corresponding mechanism has been a subject under investigation.^[13]

The study on the droplet deformation due to electrostatic stresses starts when Taylor^[14] introduced the leaky dielectric model to describe small droplet deformation under weak electric fields. The shortcoming of this theory is that the prediction deviates from the experimental data when the deformation is large. To make up this weakness, an extended leaky dielectric model has been proposed for large droplet deformation in electric fields.^[15] It is noticeable that the above theoretical analysis only obtains solutions for the stable state while the droplet experiences a transient deformation process. Against this insufficiency, Dubash and Mestel^[16] developed a transient deformation theory for electrohydrostatics deformation cases, while Lin *et al.*^[17] employed the full Taylor–Melcher leaky dielectric model to solve the transient electrohydrodynamics problem as the finite charge relaxation time is provided. However, their theoretical analysis comes across some difficulties

in predicting the periodic oscillation deformation which is often found in the experiments.

Accompany with the development of theoretical method, some experimental researches have been devoted to revealing the deformation mechanisms of droplet under electric fields. Allan and Mason^[18] performed the experiments to investigate the droplet deformation suspended in liquid dielectrics at low electric fields, which showed good quantitative agreement with theoretical equations based on electrostatic theory. Later, Torza *et al.*^[19] experimentally studied the prolate/oblate deformation of droplet in electric fields, while the experiments of Tsukada's group^[20] focused on the small droplet deformation and predicted the deformation with the finite element method. Note that the experiments mentioned above mainly concerned the droplet behaviors of relatively small droplet deformation in the electric fields such as prolate deformation or oblate deformation. If the droplet deforms under a stronger electric field, more complex behaviors will be observed. For example, Ha *et al.*^[21] found the existence of droplet rotation mode and proposed the electric capillary number to analyze the critical fracture mode under DC electric fields. Sato *et al.*^[22] experimentally studied the deformation and fracture process of droplets in a uniform electric field, and found five different behavior modes of droplets and their appearing conditions.

Although some quantitative studies on the rotational behaviors of droplets have been reported, quantitative studies on the other electrodynamic behaviors of droplets are still scarce.^[20,23,24] Especially when the dimensionless function

*Project supported by the National Natural Science Foundation of China (Grant Nos. 51725602 and 51906039) and the Natural Science Foundation of Jiangsu Province, China (Grant No. BK20180405).

†Corresponding author. E-mail: iamyucheng@seu.edu.cn

$RS < 1$, the unsteady evolution of the droplet under the DC electric field has not been fully revealed. Here, R and S are the dimensionless parameters which can be written as

$$R = \frac{\kappa_2}{\kappa_1}, \quad S = \frac{\varepsilon_1}{\varepsilon_2}, \quad (1)$$

where κ is the conductivity, ε is the dielectric constant, subscript 1 denotes the outer fluid, and subscript 2 denotes the droplet fluid. In this context, silicone oil and castor oil are used as droplet fluid and outer fluid, respectively. The behaviors of single silicone oil droplet under electric fields are experimentally studied and the different behavior modes can be found. Moreover, the non-steady-state evolution process of droplets is also demonstrated under electric fields. The effect of different working conditions on the behavior modes is analyzed.

2. Experimental section

As shown in Fig. 1, the experimental system consists of a high-voltage power supply (maximum output voltage of 30 kV,

model: P303M1E), electric field trough and high-speed visualization microscopy system. The electric field trough is composed of transparent acrylic glass, where two parallel brass plates are fixed on the inner wall as positive and negative electrodes. The size of the brass plate is set to 5 cm×5 cm and their distance is 2 cm, which are respectively connected to the positive and negative electrodes of the high-voltage DC power supply. Thus, the parallel plate electric field can be constructed with the spatial uniformity and reduce the influence of the electric field line distortion. The high-speed visualization microscopy system consists of a high speed charge coupled device (CCD) and a microscope, which can monitor the electrodynamic behavior of droplet under different operating conditions in real time. The physical properties of the fluids are presented in Table 1. The electric field trough is filled with castor oil to build a capacitor, and a silicone oil droplet is placed in the castor oil through a pipette.

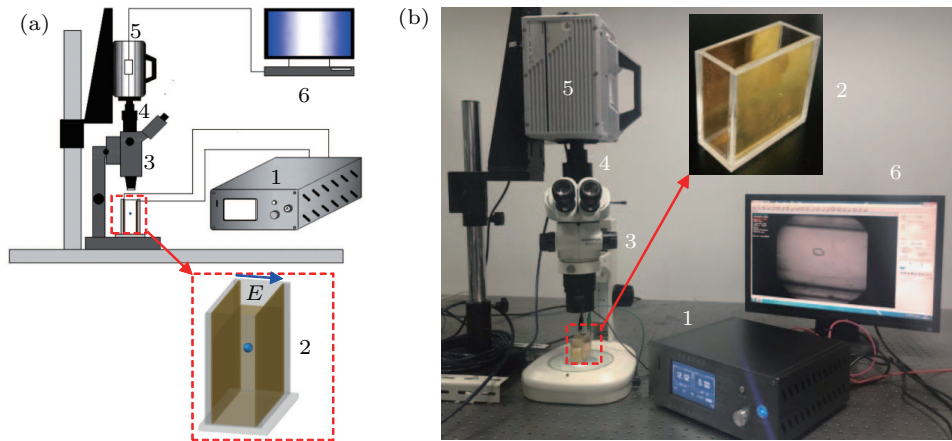


Fig. 1. Experimental setup: (a) schematic diagram; (b) corresponding physical diagram (1: high voltage power supply; 2: electric field trough; 3: microscope; 4: transformer; 5: high speed CCD; 6: computer).

Table 1. Physical parameters.

	Working fluid	Density/(g/cm ³)	Relative permittivity	Conductivity/(S/m)	Viscosity/(Pa·s)
Outer fluid	castor Oil	0.955	5.3	4.5×10^{-11}	0.71
	silicone oil (50 cSt)	0.960	3.0	1.23×10^{-12}	0.05
Droplet fluid	silicone oil (500 cSt)	0.970	3.0	1.23×10^{-12}	0.49
	silicone oil (1000 cSt)	0.971	3.0	1.23×10^{-12}	0.97

3. Experiment validation

In order to verify reasonability of working conditions, several kinds of droplets with different viscosities are prepared in the experiments, and the experimental results are compared with the theoretical ones.^[24] In Figs. 2(a)–2(c), the relative electric field strength and interfacial tension which are expressed by the dimensionless electric capillary number Ca_E can be written as

$$Ca_E = \frac{a\varepsilon_1 E_0^2}{2\gamma}, \quad (2)$$

where a is the initial diameter of the droplet, γ is the interfacial tension of the inner and outer fluids, E_0 is the electric field strength. The degree of deformation D can be written as

$$D = \frac{d_p - d_v}{d_p + d_v}, \quad (3)$$

where d_p is the length of the axis parallel to the direction of the electric field, d_v is the length of the axis perpendicular to the direction of the electric field.^[14] According to Taylor's small deformation theory, the degree of deformation D is linear with the electric capillary number Ca_E as follows:^[24]

$$D = \frac{9}{16S(2+R)^2} \left[S(R^2 + 1) - 2 + 3(RS - 1) \frac{2\lambda + 3}{5\lambda + 5} \right] Ca_E, \quad (4)$$

where λ is the ratio between the drop viscosity μ_2 and outer fluid viscosity μ_1 , *i.e.*, $\lambda = \mu_2/\mu_1$.

It can be seen from Fig. 2 that as Ca_E increases, D of the oblate ellipses also increases. In small region of Ca_E , the experimental values are closer to the Taylor's theoretical predictions.^[24] But after Ca_E is larger than 1, the experimental data begin to deviate significantly from the Taylor's theoretical predictions. In addition, the deviation degree between experi-

mental results and theoretical predictions is different when the inner and outer fluid viscosity ratios are inconsistent. It is due to the fact that Taylor's leaky dielectric theory ignores charge convection, which leads to inaccurate prediction of droplet deformation behavior. The charge convection has a reverse resistance to the droplet deformation and reduces the flow intensity of the electrohydrodynamics, which causes the flat elliptical deformation of the silicone oil droplet smaller than the theoretical value. In general, it proves the reasonability of working conditions of current experiment.

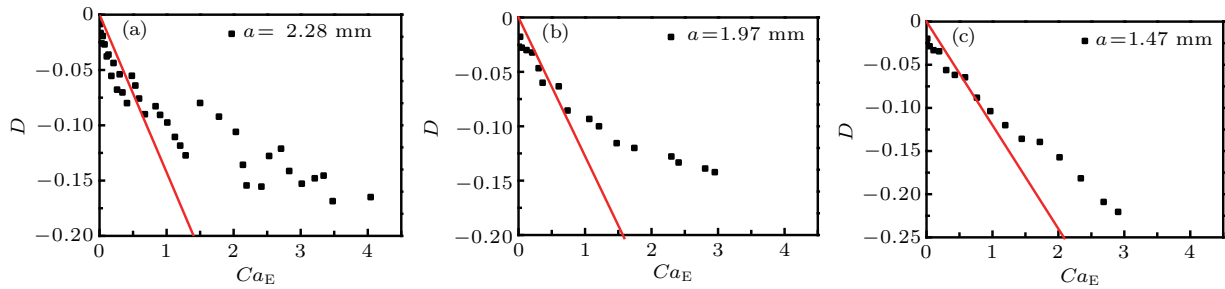


Fig. 2. Effect of Ca_E on D under different operating conditions: (a) $\lambda = 0.07$, (b) $\lambda = 0.7$, (c) $\lambda = 1.4$. The straight line is Taylor's small deformation theory curve.

4. Results and discussion

4.1. Typical behavior modes

Under the action of a uniform DC electric field, the behaviors of silicone oil droplets suspended in castor oil are mainly divided into four modes, namely Taylor deformation mode,^[14] typical oblique rotation mode,^[19,20] periodic oscillation mode,^[22,25,26] and fracture mode.^[21,22]

Figure 3(a) shows the unsteady evolution of droplets over

time in the Taylor deformation mode. When the outer electric field strength is within a certain range, the induced electric charge can overcome the interfacial tension and the pressure difference between the inside and outside of the droplet which causes Taylor deformation.^[14] The deformation degree of the droplet increases with the time increasing and the droplet will become a flat elliptical shape. At that time, the short-axis direction of the droplet is parallel to the direction of the electric field which is defined as Taylor deformation mode.

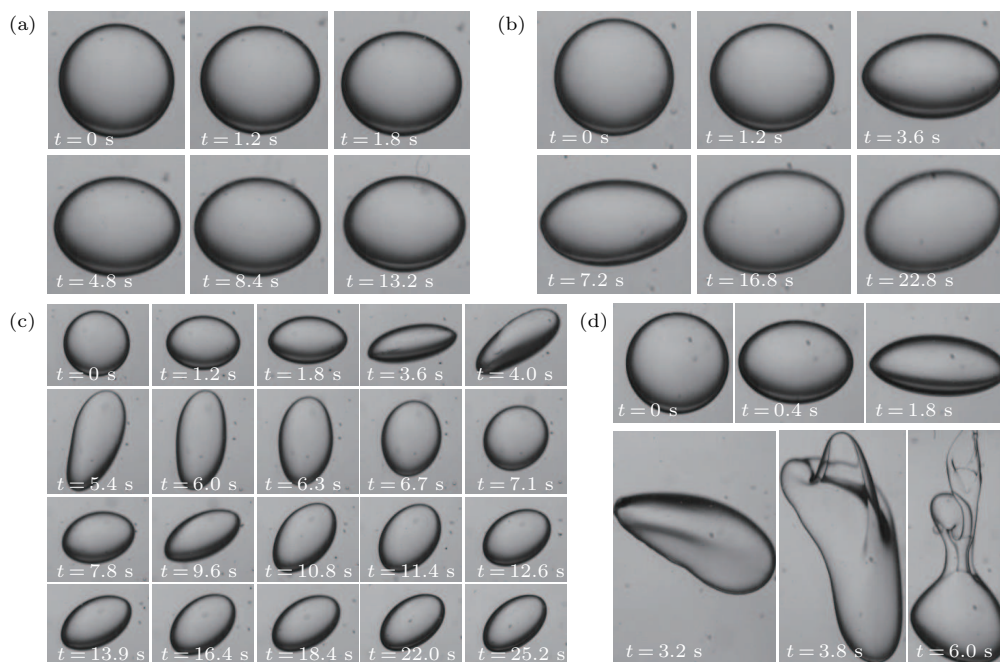


Fig. 3. Evolution of silicone oil droplets over time in different modes (viscosity ratio $\lambda = 1.4$, initial diameter $a = 3.05$ mm). (a) The deformation evolution process of droplets in Taylor deformation mode with $E_0 = 2$ kV/cm. (b) The deformation evolution process of the drop in the typical oblique rotation mode with $E_0 = 3.25$ kV/cm. (c) The evolution process of drop deformation in periodic oscillation mode with $E_0 = 3.9$ kV/cm. (d) The deformation evolution process of the drop in the fracture mode with $E_0 = 4.5$ kV/cm.

As the electric field strength increases, the flat elliptical droplet begins to become unstable. Once the electric field strength exceeds the threshold value, the droplet cannot keep stable after the flat ellipse deformation. It can be found that the droplet will rotate in the oblique direction with a certain angle between the long axis direction and the vertical electric field direction, which is defined as typical oblique rotation mode.^[27] Figure 3(b) shows the non-steady state of droplet shape over time in a typical oblique rotation mode. The threshold electric field strength of the droplet from the Taylor deformation mode to the oblique rotation mode is called the rotation critical electric field strength E_c .

As shown in Fig. 3(c), a periodic oscillation mode is observed between the typical oblique rotation mode and the fracture mode, which shows periodical changes of droplet shape. In this transition mode, the droplets undergo a cyclic oscillation process between the deformed rotation state and the elongated-contraction deformation state, and finally reach a stable state of the oblique rotation with deformation. The amplitude of the oscillation between these two states becomes smaller and smaller until the oscillation disappears, and its final steady state coincides with the typical oblique rotation

mode.

When E_0 reaches a higher value, the applied outer electric field eventually causes breakup of the droplet, which is called the fracture mode. In the fracture mode, the drop first undergoes the Taylor deformation period, then evolves to the oblique rotation phase and eventually fractures. Figure 3(d) shows the unsteady state of the droplet shape over time in the fracture mode.

4.2. Deformation parameters in different modes

4.2.1. Effect of electric field strengths on D and α in Taylor deformation mode

In the Taylor deformation mode, when the applied outer electric field is within the critical electric field strength, the force of the outer electric field on the induced electric charge overcomes the interfacial tension and the inner and outer pressure difference. Thus, the droplet can produce a flat elliptical deformation which causes the short axis direction to be parallel to the electric field direction. Subsequently, the deformation degree of the silicone oil droplet increases and eventually tends to a steady state.

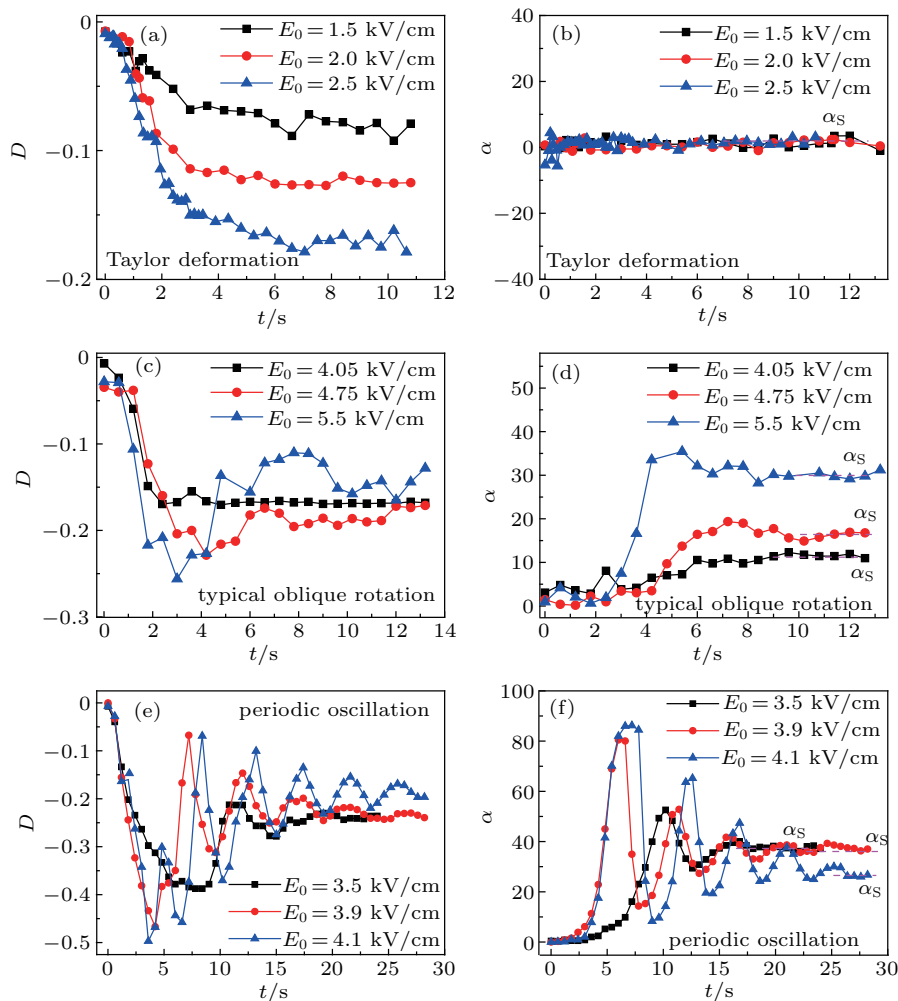


Fig. 4. (a) and (b) The effect of electric field strengths on D and α in Taylor deformation mode with $\lambda = 1.4$, $a = 3.05$ mm. (c) and (d) The effect of electric field strengths on D and α in typical oblique rotation mode with $\lambda = 1.4$, $a = 1.24$ mm. (e) and (f) The effect of electric field strengths on D and α in the periodic oscillation mode with $\lambda = 1.4$, $a = 3.05$ mm. α_s denotes the steady-state rotation angle.

Figures 4(a) and 4(b) show the effect of three different electric field strengths which are below the critical electric field on degree of deformation D ^[14] and rotation angle α . The rotation angle α is the angle between the long axis direction of the oblate ellipses and the direction of the vertical electric field. It can be seen that firstly D increases rapidly in a short time after applying a DC electric field, and then the growth rate becomes slower, and finally D gradually keeps into a fixed value. Moreover, it is demonstrated that, under the same viscosity ratio and initial size, the higher the electric field strength can produce the larger the force which is applied by the outer electric field, and the larger D in the final steady state. It is worth noting that the silicone oil droplet can only deform but without rotation during the Taylor deformation.

4.2.2. Effect of electric field strengths on D and α in typical oblique rotation mode

As the electric field strength exceeds the critical value, rotation disturbance occurs at that time and the flat elliptical deformed droplet becomes unstable. After undergoing Taylor deformation, the droplet begins to rotate toward the oblique direction whose long axis direction and the vertical electric field direction appear at a certain angle and maintain the steady state, and enter the oblique rotation phase with deformation. Figures 4(c) and 4(d) show the effect of electric field strengths on D and α in typical oblique rotation mode. It can be seen that higher electric field strength can cause larger D and α at the final steady state. But once the droplet starts to rotate, D will decrease to some extent and the larger electric field strength can promote larger reduction of D . In the final steady state condition, D will keep almost unchanged as the electric field strength increases.

4.2.3. Effect of electric field strengths on D and α in periodic oscillation mode

In the periodic oscillation mode, the droplet does not immediately maintain the steady state but undergoes a transition mode with periodical shape changes of droplet. In this transition mode, the droplet undergoes a cyclic oscillation process between the deformed rotation state and the elongated-contraction deformation state, and finally reach a stable state of the oblique rotation with deformation. Figures 4(e) and 4(f) show the effect of electric field strengths on D and α in the periodic oscillation mode. After applying the DC electric field, D will increase at the first short time and α remains unchanged at around zero. Then α will increase sharply and D still keeps stable. Finally, the droplet keeps at a certain D and α after a period of oscillation.

4.3. Effect of different working conditions parameters

Figure 5 presents the dimensionless critical electric field strength E_c/E_Q with different initial diameter and viscosity

of droplet. E_Q is the theoretical critical rotating electric field strength of rigid sphere and described as^[24]

$$E_Q^2 = \frac{2\kappa_1\mu_1(R+2)^2}{3\epsilon_1\epsilon_2(1-RS)}. \tag{5}$$

As shown in the figure, the decrease of viscosity of droplet leads to an increasing critical rotating electric field strength. In addition, the increase of droplet size can cause the decrease of critical electric field strength at the same viscosity ratio. Besides, the effect of drop diameter is much smaller than viscosity.

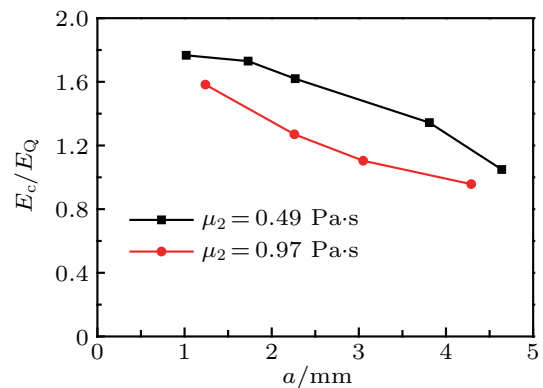


Fig. 5. The dimensionless critical electric field strength E_c/E_Q with different initial diameter a and viscosity of droplet μ_2 .

In the oblique rotation mode, the droplets sequentially undergo flat elliptical deformation and oblique rotation with deformation and finally maintain a steady-state rotation angle α_S . However, the rotation angle can change under different electric field strength E_0 . The final stable rotation angle of the droplet is related to the electric field strength, droplet size, inner and outer fluid viscosity ratio. Figure 6 presents the steady-state rotation angle α_S of the droplet with the electric field strength E_0 when $\lambda = 1.4$. It can be seen that a higher electric field strength leads to larger steady-state rotation angle when the droplet is stable. Additionally, it can be found that the smaller droplet size can cause greater change of the steady-state rotation angle.

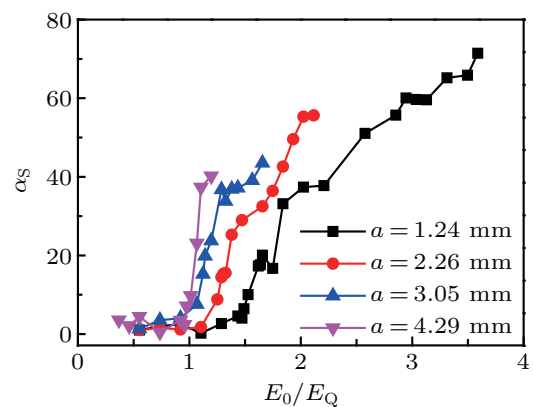


Fig. 6. The steady-state rotation angle α_S of the droplet with different dimensionless electric field strength E_0/E_Q when $\lambda = 1.4$.

5. Conclusion

In this paper, a high-speed visualization microscopic observation platform for the dynamic behavior of droplets under uniform DC electric field is established. The different dynamic behavior modes and evolution processes of silicone oil droplets in castor oil under uniform DC electric fields are experimentally studied. Moreover, the effect of different working conditions (such as electric field strength, droplet diameter, etc.) on droplet behavior can be found. Through this visualization experiment, the main conclusions can be listed as follows:

(i) The electrohydrodynamic behaviors of silicone oil droplets in castor oil fluid under DC electric fields can be divided into four modes: Taylor deformation, typical oblique rotation, periodic oscillation and fracture. The mode transition occurs with the increase of electric field strength.

(ii) The experimental value of D is closer to the Taylor theoretical prediction value when the electric capillary is small. The experimental data begins to significantly deviate from the theoretical prediction when Ca_E is larger than 1. In addition, higher viscosity ratio can induce small deviation from the theoretical value.

(iii) The critical electric field strength of rotation increases with the decrease of viscosity ratio and the droplet size, but the droplet size has little effect compared with the viscosity ratio.

(iv) The higher electric field strength and smaller droplet size can cause larger rotation angle when the droplet is finally

stabilized.

References

- [1] Ha J W and Yang S M 1998 *J. Colloid. Interf. Sci.* **206** 195
- [2] Melcher J R and Taylor G I 1969 *Ann. Rev. Fluid Mech.* **1** 111
- [3] Zhang C B, Gao W, Zhao Y J and Chen Y P 2018 *Appl. Phys. Lett.* **113** 203702
- [4] Chen Y, Gao W, Zhang C and Zhao Y 2016 *Lab. Chip* **16** 1332
- [5] Huang H, Hong N, Liang H, Shi B C and Chai Z H 2016 *Acta Phys. Sin.* **65** 084702 (in Chinese)
- [6] Feng J Q 1999 *Proc. R. Soc. A* **455** 2245
- [7] Stone H A 1994 *Ann. Rev. Fluid Mech.* **26** 65
- [8] Wang J, Gao W, Zhang H, Zou M H, Chen Y P and Zhao Y J 2018 *Sci. Adv.* **4** eaat7392
- [9] Shkadov V Y and Shutov A A 2002 *Fluid Dyn.* **37** 713
- [10] Zhang C, Yu F, Li X and Chen Y 2019 *AIChE J.* **65** 1119
- [11] Chen Y, Zhang C, Shi M and Yang Y 2010 *AIChE J.* **56** 2018
- [12] Cui Y, Wang N and Liu H 2019 *Phys. Fluids* **31** 022105
- [13] Nishiwaki T, Adachi K and Kotaka T 1988 *Langmuir* **4** 170
- [14] Taylor G 1966 *Proc. R. Soc. Lond. A* **291** 159
- [15] Benteñitis N and Krause S 2005 *Langmuir* **21** 6194
- [16] Dubash N and Mestel A J 2007 *J. Fluid Mech.* **581** 469
- [17] Das S P and Yoshimori A 2013 *Phys. Rev. E* **88** 043008
- [18] Allan R S and Mason S G 1962 *Proc. R. Soc. Lond. A* **267** 45
- [19] Torza S, Cox R G and Mason S G 1971 *Philos. Trans. R. Soc. London Ser. A* **269** 295
- [20] Tsukada T, Katayama T, Ito Y and Hozawa M 1993 *J. Chem. Eng. Jpn.* **26** 698
- [21] Ha J W and Yang S M 2000 *Phys. Fluids* **12** 764
- [22] Sato H, Kaji N, Mochizuki T and Mori Y H 2006 *Phys. Fluids* **18** 127101
- [23] Dodgson N and Sozou C 1987 *Z. Angew. Math. Phys.* **38** 424
- [24] Salipante P F and Vlahovska P M 2010 *Phys. Fluids* **22** 112110
- [25] Salipante P F and Vlahovska P M 2013 *Phys. Rev. E* **88** 043003
- [26] Vlahovska P M 2016 *Phys. Rev. Fluids* **1** 060504
- [27] Jones T B 1984 *IEEE T. Ind. Appl.* **20** 845